New Phytologist

Research

Insights from *in vivo* micro-CT analysis: testing the hydraulic vulnerability segmentation in *Acer pseudoplatanus* and *Fagus sylvatica* seedlings

Adriano Losso[1], Andreas Bär[1], Birgit Dämon[1], Christian Dullin[2,3,4], Andrea Ganthaler[1], Francesco Petruzzellis[5], Tadeja Savi[6], Giuliana Tromba[4], Andrea Nardini[5], Stefan Mayr[1] and Barbara Beikircher[1]

[1]Department of Botany, University of Innsbruck, Sternwarterstrasse 15, Innsbruck A-6020, Austria; [2]Institute for Diagnostic and Interventional Radiology, University Medical Center Goettingen, Robert-Koch-Straße 40, Göttingen 37075, Germany; [3]Max-Plank-Institute for Experimental Medicine, Hermann-Rein-Straße 3, Göttingen 37075, Germany; [4]Elettra-Sincrotrone Trieste, Area Science Park, Trieste, Basovizza 34149, Italy; [5]Dipartimento di Scienze della Vita, Università di Trieste, Via L. Giorgieri 10, Trieste 34127, Italy; [6]Department of Crop Sciences, Division of Viticulture and Pomology, University of Natural Resources and Life Sciences Vienna, Konrad Lorenzstrasse 24, Tulln A-3430, Austria

Author for correspondence:
Adriano Losso
Tel: +43 650 3126709
Email: adriano.losso@uibk.ac.at

Received: *18 April 2018*
Accepted: *14 October 2018*

New Phytologist (2019) **221:** 1831–1842
doi: 10.1111/nph.15549

Key words: beech (*Fagus sylvatica*), embolism, hydraulic vulnerability segmentation, maple (*Acer pseudoplatanus*), seedlings, synchrotron, X-ray phase contrast micro-tomography (micro-CT), xylem.

Summary

- The seedling stage is the most susceptible one during a tree's life. Water relations may be crucial for seedlings due to their small roots, limited water buffers and the effects of drought on water transport. Despite obvious relevance, studies on seedling xylem hydraulics are scarce as respective methodical approaches are limited.
- Micro-CT scans of intact *Acer pseudoplatanus* and *Fagus sylvatica* seedlings dehydrated to different water potentials (Ψ) allowed the simultaneous observation of gas-filled versus water-filled conduits and the calculation of percentage loss of conductivity (PLC) in stems, roots and leaves (petioles or main veins). Additionally, anatomical analyses were performed and stem PLC measured with hydraulic techniques.
- In *A. pseudoplatanus*, petioles showed a higher Ψ at 50% PLC (Ψ_{50} −1.13MPa) than stems (−2.51 MPa) and roots (−1.78 MPa). The main leaf veins of *F. sylvatica* had similar Ψ_{50} values (−2.26 MPa) to stems (−2.74 MPa) and roots (−2.75 MPa). In both species, no difference between root and stems was observed. Hydraulic measurements on stems closely matched the micro-CT based PLC calculations.
- Micro-CT analyses indicated a species-specific hydraulic architecture. Vulnerability segmentation, enabling a disconnection of the hydraulic pathway upon drought, was observed in *A. pseudoplatanus* but not in the especially shade-tolerant *F. sylvatica*. Hydraulic patterns could partly be related to xylem anatomical traits.

Introduction

Trees can live for hundreds of years, sometimes facing and resisting very harsh environmental conditions during their life span. Yet, the most critical and threatening stages in a tree's life can be tracked back to the very few weeks after seed germination. At the seedling stage, the plant relies upon reserves stored in the seed, until cotyledons unfold and start to perform active photosynthesis. Seedlings and the following juvenile stages are at a very high risk of death (e.g. Fenner, 1987; Larcher, 2003; Smith *et al.*, 2003; Johnson *et al.*, 2011), because productivity and reserves are small, investments in growing organs have to be perfectly balanced and respective sensitivity to many biotic and abiotic stress factors is high. Water relations are key issues during early ontogeny as root systems are small and shallow, water supply relies on upper soil layers, which are easily exposed to dehydration, and internal water buffers are limited. Despite the small size and relatively short transport distances, multiple studies have indicated that transport hydraulic efficiency and safety of seedlings play a central role in plant survival, just like in adult trees (e.g. Grulke & Retzlaff, 2001; Rice *et al.*, 2004; Domec *et al.*, 2009). Moreover, the increasing frequency and intensity of drought events (e.g. Sperry & Love, 2015) are limiting the establishment and survival of plants, as seedlings play a critical role in tree population dynamics and shifts in species distributions under climate change (Ibanez *et al.*, 2007; Vanderwel *et al.*, 2013). Knowledge on seedling hydraulics, therefore, is relevant for various fields such as forestry or nature conservation.

Root-to-leaf water transport is necessary to compensate transpirational water losses (cohesion-tension theory; Boehm, 1893; Dixon & Joly, 1894; Steudle, 2001) and unavoidable generates a water potential (Ψ) gradient along the xylem pathway. The resulting negative hydrostatic pressure in xylem conduits implies the risk of embolism formation and propagation in the xylem

(Tyree & Zimmermann, 2002). Embolism causes blockages in xylem conduits that, in turn, reduce plant hydraulic conductance, limit photosynthesis and can even lead to plant death (e.g. Brodribb & Cochard, 2009). Embolism can result from drought stress, when low Ψ cause the aspiration of gaseous bubbles into xylem conduits from adjacent gas-filled compartments via the pits (air seeding; Tyree & Zimmermann, 2002; see also Choat *et al.*, 2015, 2016). Low Ψ is also responsible for embolism formation when plants are exposed to freeze–thaw cycles (e.g. Pittermann & Sperry, 2003; Mayr & Sperry, 2010).

In adult trees, the xylem vulnerability to embolism can differ both between (e.g. Choat *et al.*, 2012) and within species (e.g. Beikircher & Mayr, 2009), as well as between organs of specimens (e.g. Tsuda & Tyree, 1997; Beikircher *et al.*, 2013; Scholz *et al.*, 2014; Johnson *et al.*, 2016). It has been suggested that within-plant variation in vulnerability follows distinct patterns, with distal plant parts, such as leaves or small branches, being more vulnerable to drought-induced xylem embolism than central and older parts, such as the trunk (hydraulic vulnerability segmentation hypothesis; Tyree & Ewers, 1991; Tyree & Zimmermann, 2002). This would enable drought stressed plants to sacrifice highly vulnerable plant segments by confining embolism in the distal sectors, while keeping the remaining parts hydraulically active and therefore protecting central parts of the water transport system with high carbon investments (e.g. trunk and larger stems). In angiosperms, many studies demonstrated petioles and leaves to be more vulnerable than branches (Tyree *et al.*, 1993; Tsuda & Tyree, 1997; Beikircher *et al.*, 2013; Scholz *et al.*, 2014; Charrier *et al.*, 2016; Johnson *et al.*, 2016; Wolfe *et al.*, 2016). Leaves probably exhibit vulnerable extra-xylary pathways, which disconnect the xylem from distal water transport under moderate drought stress (Trifilò *et al.*, 2016; Scoffoni *et al.*, 2017). In some cases, however, trunks were reported to be more vulnerable than branches (e.g. Johnson *et al.*, 2016; Rosner *et al.*, 2018), and other studies found similar vulnerabilities across organs (e.g. Choat *et al.*, 2005; Hao *et al.*, 2013). Roots were shown to be more vulnerable than branches in several studies (e.g. Martínez-Vilalta *et al.*, 2002; Maherali *et al.*, 2006; Johnson *et al.*, 2016). Within-plant variation in vulnerability has also been reported for conifers (Kavanagh *et al.*, 1999; Beikircher & Mayr, 2008; Willson *et al.*, 2008; Domec *et al.*, 2009; Delzon *et al.*, 2010; McCulloh *et al.*, 2014; Losso *et al.*, 2016; Miller & Johnson, 2017). It is likely that vulnerability segmentation is species-specific and can show various patterns. These patterns are based on variation in xylem properties (e.g. Hacke *et al.*, 2001; Gleason *et al.*, 2016), which are known to determine the stability of the hydraulic pathway. Most important, the pit characteristics influences air-seeding thresholds (Tyree *et al.*, 1994; Li *et al.*, 2016), and the cell-wall reinforcement counterbalances maximum tension occurring in xylem conduits (Hacke *et al.*, 2001). Most studies on vulnerability segmentation dealt with adult trees (see citations above) and few on shrubs or herbs (e.g. Ganthaler & Mayr, 2015; Nolf *et al.*, 2016; Savi *et al.*, 2016; Skelton *et al.*, 2017), while studies on youngest tree stages (i.e. < 1 yr old) are scarce (Rodriguez-Dominguez *et al.*, 2018). To our knowledge, there are only two studies that directly measured hydraulic vulnerability (Lauenstein *et al.*, 2013; Way *et al.*, 2013) and none on hydraulic segmentation dealing with plants of an age up to 6 months. This is related to methodical limitations as hydraulic measurements on small plants are difficult. Fortunately, new methods now enable studies on samples of small size, such as the seedlings analysed in the present study.

In past years, a wide variety of experimental techniques has been developed and used for measuring the vulnerability to drought-induced xylem embolism of different plant organs (Cochard *et al.*, 2013). In particular, noninvasive *in vivo* visualisation techniques have recently taken hold in the field of plant hydraulics (e.g. Choat *et al.*, 2010; Cochard *et al.*, 2015; Jansen *et al.*, 2015; Brodribb *et al.*, 2016). X-ray phase contrast micro-tomography (micro-CT) is so far the most promising method, as it is nondestructive (but see Petruzzellis *et al.*, 2018) and allows *in vivo* observations of conduits status (in terms of water- vs air-filled conduits) and thus to analyse hydraulic integrity and embolism patterns within organs (e.g. Brodersen *et al.*, 2013; Choat *et al.*, 2015). This technique provides the possibility to visualise at high resolution and quantify xylem embolism in detached branches (e.g. Cochard *et al.*, 2015; Choat *et al.*, 2016; Knipfer *et al.*, 2016; Nardini *et al.*, 2017), leaves (Bouche *et al.*, 2016; Ryu *et al.*, 2016; Scoffoni *et al.*, 2017), roots (Cuneo *et al.*, 2016) as well as on the main stem of intact plants (Choat *et al.*, 2015; Knipfer *et al.*, 2017; Nolf *et al.*, 2017; Savi *et al.*, 2017).

In the present study, we used synchrotron-based micro-CT to analyse the vulnerability to drought-induced xylem embolism of 6-month-old *Acer pseudoplatanus* and *Fagus sylvatica* plants (here after called seedlings). The study aimed at real-time observations of xylem conduits in main organs (stem, roots and leaves) during progressive plant dehydration. Based on the micro-CT technique, it was not only possible to study intact seedlings but also to compare vulnerability patterns within single plants. We designed an experiment that enabled simultaneous micro-CT observations at multiple points in intact plants and thus recording within-plant vulnerability patterns with respect to main roots, stems, petioles or leaf veins. We also compared the theoretical loss of stem hydraulic conductivity (PLC_t) calculated from micro-CT observations with classical hydraulic measurements performed on seedling stems, which is important in the view of recent methodical controversies (e.g. Wheeler *et al.*, 2013; Trifilò *et al.*, 2014; Venturas *et al.*, 2015). A comparison between hydraulic and micro-CT methods on identical plant material has been done in only three recent studies, in which Nardini *et al.* (2017) and Nolf *et al.* (2017) demonstrated agreement between methods, while Savi *et al.* (2017) highlighted possible discrepancies.

We hypothesised that seedlings show pronounced and species-specific patterns in vulnerability to drought-induced embolism, with higher hydraulic safety in the main stem compared with leaves and overall small safety in roots. Roots are exposed to overall less negative Ψ as they are situated in the basal part of the soil–plant continuum and accordingly, comparably low hydraulic safety was reported for roots of mature trees (see the third paragraph of the Introduction). Furthermore, we expected similar vulnerability curves from micro-CT and hydraulic measurements

performed using standard protocols. This micro-CT study should improve our knowledge of xylem hydraulic safety in seedlings, an important aspect in the youngest stage of a tree's life.

Materials and Methods

All experiments were conducted in September and October 2017 on 6-month-old seedlings of *Acer pseudoplatanus* L. and *Fagus sylvatica* L. Seeds (Herzog.Baum, Samen und Pflanzen GmbH, Gmunden, Austria) were sown in small pots (8 cm high and 7 cm wide; to allow an easy handling during experiments). For optimal growing conditions, plants were placed in a glasshouse and constantly irrigated to field capacity (every 2–3 d). At the time of measurements, seedlings were *c.* 15–20 cm tall with a stem diameter of 3–4 mm. Micro-CT measurements were performed on the following plant organs: stems, main roots (all seedlings had a main root, which was thicker than the others; *c.* 0.5–0.8 mm in diameter), petioles (*A. pseudoplatanus*) and main leaf veins (*F. sylvatica*). Hydraulic measurements were performed only on stems.

Hydraulic measurements

Vulnerability to drought-induced xylem embolism was measured hydraulically using the 'bench dehydration' technique (Sperry *et al.*, 1988; Cochard *et al.*, 2013). Fully hydrated seedlings were removed from pots, and roots were carefully rinsed to remove soil residuals. Seedlings were left dehydrating to different water potentials (Ψ) in the laboratory (time intervals ranging between 20 min to 8 h). To allow equilibration of Ψ within plants and obtain accurate Ψ measurements, seedlings were then wrapped in dark plastic bags for 30–45 min before measurement. After dehydration, the apical part of the seedling (3–5 cm including leaves) was used to measure Ψ (Scholander apparatus model 1505D; PMS Instruments, Albany, OR, USA). Out of the central part of the stem, an *c.* 6 cm long sample was cut under water, the bark was removed and the sample trimmed several times with a sharp carving knife to gradually release tension, remove micro-bubbles (Wheeler *et al.*, 2013; Venturas *et al.*, 2015) and minimize eventual artefacts due to xylem refilling under rehydration (Trifilò *et al.*, 2014). Samples were then connected to a modified Sperry apparatus (Sperry *et al.*, 1988; Losso *et al.*, 2018) and perfused with distilled and degassed water, filtered at 0.2 µm and containing 0.005% (v/v) Micropur (Katadyn Products, Wallisellen, Switzerland) to prevent microbial growth. The initial hydraulic conductivity (K_i; normalised by xylem cross-sectional area and sample length) was measured at 4 kPa. *F. sylvatica* samples were then flushed for 10 min at 60 kPa to remove embolism. After flushing, the hydraulic conductivity was measured again. Flushing was repeated until measurements showed no further increase in conductivity to obtain final specific hydraulic conductivity (also normalised by xylem cross-sectional area and sample length; K_s). All hydraulic measurements were conducted at room temperature (*c.* 21–22°C). Conductivity values were corrected for water viscosity at 20°C, and percent loss of conductivity (PLC) was calculated as:

$$\mathrm{PLC} = \left(1 - \frac{K_i}{K_s}\right) \times 100 \qquad \text{Eqn 1}$$

For *A. pseudoplatanus*, direct measurements of PLC were not possible as conductivities progressively decreased upon flushing, indicating conduit plugging. Therefore, PLC was calculated from the conductivity of dehydrated samples (corresponding to K_i in Eqn 1) vs the conductivity of saturated samples (Ks in Eqn 1; Beikircher & Mayr, 2009). *F. sylvatica* dehydrated very rapidly at Ψ between *c.* −2 to −4 MPa so that only few data points could be measured in this range. Respective vulnerability curves thus show gaps, but determination of vulnerability thresholds was still possible due to sufficient measurements below and above the critical range and to a sufficient number of replicates.

PLC was plotted vs the corresponding Ψ and a Weibull regression curve was fitted to each vulnerability curve (R-package FIT-PLC, R i386 3.2.5; Duursma & Choat, 2017). From vulnerability plots, we also extracted the thresholds Ψ_{12}, Ψ_{50} and Ψ_{88}, which refer to Ψ at 12%, 50% and 88% loss of conductivity, respectively (Domec & Gartner, 2001; Choat *et al.*, 2012).

Micro-CT observations

Micro-CT scans were performed at the SYRMEP beamline of the Elettra Light Source in Trieste, Italy (Tromba *et al.*, 2010) using the propagation-based phase contrast technique. Seedlings were transported to the facility and stored at a shaded field site until preparation for the analyses. Plants were carefully removed from the pots and roots carefully rinsed to remove soil residuals before bench dehydration (as described above in 'Hydraulic measurements'). To simultaneously observe the functional status of xylem conduits in three different organs (stem, main root and leaf), seedlings were prepared as shown in Fig. 1. Briefly, the main root and a leaf were bent upwards and downwards, respectively, and positioned next to the stem. The section to be scanned (stem, leaf vein or leaf petiole, root) was wrapped in Parafilm®, while the remaining leaves and roots were wrapped in cling film to prevent further dehydration of the sample during scans. For *A. pseudoplatanus*, the petiole was observed. In the case of *F. sylvatica*, due to the short petiole, the main vein of the leaf was observed. Organs were stabilised during scan rotation using a V-shaped custom-made sample holder. This allowed an easy and fast positioning of the samples (see Fig. 1), which were fixed to the holder with Terostat putty (Teroson, Heidelberg, Germany). Thanks to the use of this sample holder, we could avoid long exposition to irradiation during the initial sample alignment, thus minimizing eventual X-ray induced cellular damage (Savi *et al.*, 2017; Petruzzellis *et al.*, 2018). Overall, sample preparation, initial alignment and scan time (90 s) were performed within 10–15 min. The scanned region of the stem was at *c.* 5–7 cm above the root collar (corresponding to stem sections used for hydraulic measurements), and at a distance of 12 cm from the detector. The field of view was 5 × 5 mm and covered the full cross-section

New Phytologist

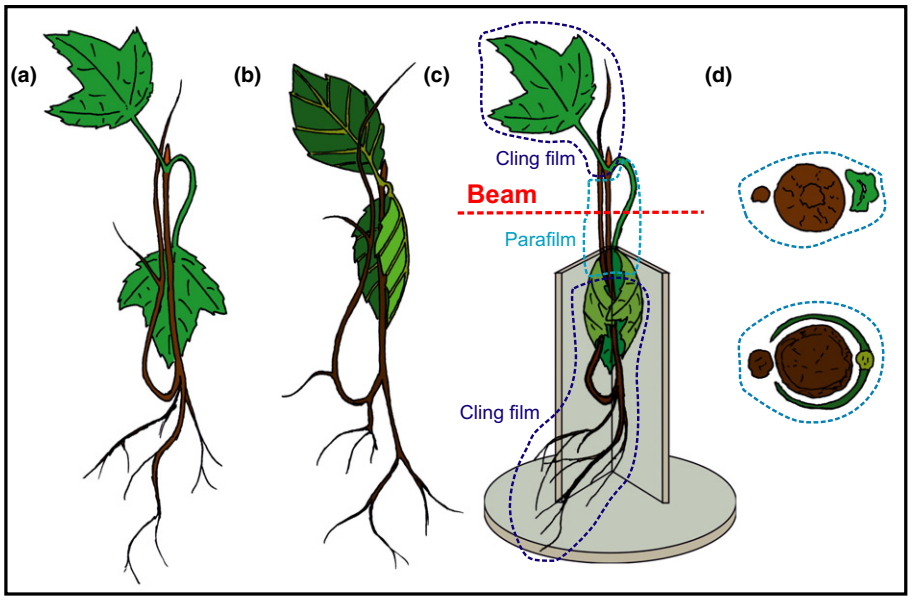

Fig. 1 Design of the sample preparation for scanning. The main root and a leaf of *Acer pseudoplatanus* (a) and *Fagus sylvatica* (b) seedlings were bent upwards and downwards, respectively, to bring them at the scanning level of the stem (4–5 cm above the root collar) and wrapped in Parafilm®. Remaining parts were wrapped in cling film (to avoid water loss during scanning) and plants placed in a custom-made sample holder (c). All three organs (stem, root and petiole/main vein) were irradiated and scanned simultaneously (d; *A. pseudoplatanus* and *F. sylvatica* in the upper and lower figure, respectively).

of the three organs. Two 5-mm filters of silicon were used to obtain an average X-ray source energy of 25 keV. The exposure time was set to 100 ms, at an angular step of $2° s^{-1}$. During the 180° rotation of the sample, 900 projections were acquired. In total, 15 seedlings of *A. pseudoplatanus* and 16 seedlings of *F. sylvatica* at different Ψ were scanned (initial scan). As for hydraulic measurements, in *F. sylvatica*, only few scans were possible between −2 and −4 MPa (see 'Hydraulic measurements'). After scans, the plant was cut directly above the root collar and Ψ of the upper part (main stem and leaves) was measured with a portable pressure chamber (3005 Plant Water Status Console; Soilmoisture Equipment Corp., Goleta, CA, USA). Stem Ψ was expected to be close to measured Ψ as plants were wrapped in cling film for 20 min at a minimum, which enabled Ψ equilibration. Finally, stem, root and petiole/leaf segments (still wrapped in Parafilm®) were cut to *c.* 4 cm length to induce air-entrance. After 24 h of dehydration, these samples were recut to 1-cm-long pieces and arranged in a row along a skewer (four samples per skewer). We then rescanned all samples at the marked position of the first scan to observe fully embolised xylem. Arrangement of several samples in a row enabled time-efficient consecutive scans by adjusting the stage height (after positioning of the first sample in the beam).

In total, 1400 slices per sample with a pixel size of 2 µm, were reconstructed using the software SYRMEP TomoProject (STP; Brun *et al.*, 2015). In STP, a phase retrieval preprocessing filter (Paganin *et al.*, 2002) was applied before the reconstruction using the Filtered Back Projection algorithm. For each sample, one central slice per sample from the initial scan and one from the final scan were analysed using IMAGEJ 1.51Q software (National Institute of Health, Bethesda, MD, USA). Images were processed to set thresholds and select only air-filled vessels (black; Fig. 2), whose areas were measured using the 'Analyse particles' function. We quantified the vessel density (VD) and the mean diameter (d) of each vessel (calculated from its area and assuming circular shape), which was used to calculate the mean hydraulic diameter (d_h) as $\Sigma d^2/\Sigma d^4$ (Kolb & Sperry, 1999) per sample and organ. To check for variation in conduit size across plant organs, we also analysed the conduit diameter distribution (2 µm classes). d was also used to calculate the theoretical hydraulic conductance (k_t). k_t is the cumulative hydraulic conductance of all conduits, which was calculated based on a modified Hagen-Poiseuille equation (e.g. Knipfer *et al.*, 2015; Cuneo *et al.*, 2016):

$$k_t = \frac{\pi\rho}{128\mu}\sum_{i=1}^{n} d_i^4 \qquad \text{Eqn 2}$$

where ρ and µ are the density of the fluid and the viscosity of water, respectively. k_t was then divided by the cross-sectional xylem area to obtain the theoretical specific hydraulic conductivity (K_{st}).

The theoretical percentage loss of hydraulic conductivity (PLC_t) was calculated by relating the initial theoretical conductivity ($K_{t\ initial}$) to the theoretical conductivity calculated from all visible conduits in the final scan ($K_{t\ final}$):

$$PLC_t = \left(1 - \frac{K_{t\,initial}}{K_{t\,final}}\right) \times 100 \qquad \text{Eqn 3}$$

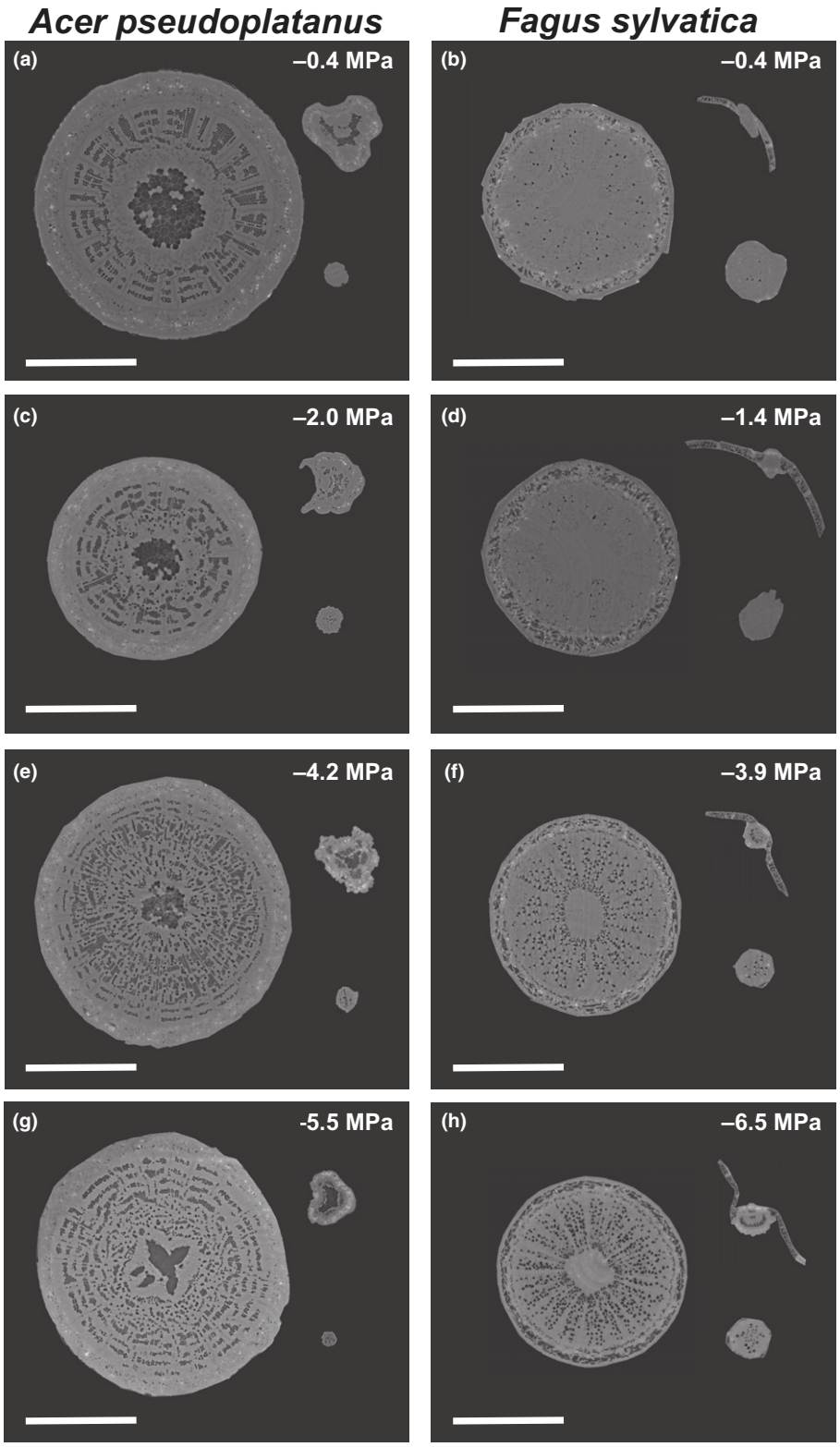

Fig. 2 *In vivo* visualization by micro-CT of xylem embolism in stems (left in each panel), leaves (petiole/main vein; upper right in each panel) and roots (lower right in each panel) in intact *Acer pseudoplatanus* (a, c, e, g) and *Fagus sylvatica* (b, d, f, h) seedlings. Reconstructed cross-sections show embolised (dark grey) and water-filled (light grey) xylem conduits at different xylem water potential (MPa). Bars, 1250 μm.

whereby $K_{t\ initial}$ was calculated from $K_{t\ final}$ minus K_t of embolised vessels in the initial scan. PLC_t was plotted vs the corresponding Ψ. Exponential sigmoid functions were fitted to each vulnerability curve (see 'Hydraulic measurements') and vulnerability thresholds were determined.

Cell-wall reinforcement

Samples used for micro-CT analyses were soaked in an ethanol/glycerol/water solution (1 : 1 : 1, v/v/v) for at least 5 d. Transversal sections were cut with a sliding microtome (Sledge Microtome

G.S.L. 1; Schenkung Dapples, Zürich, Switzerland), stained with Etzold FCA mixture (consisting of fuchsine, chrysoidine and astrablue) for 5 min and then rinsed with distilled water. From images captured with a light microscope (Olympus BX41; Olympus Austria, Wien, Austria) connected to a digital camera (ProgRes CT3; Jenoptik, Jena, Germany), we estimated the conduit wall reinforcement by calculating the 'thickness-to-span ratio' $(t/b)^2$ (Hacke *et al.*, 2001) on at least 8–10 conduit pairs per sample. The wall thickness (t) and the lumen breadth (b) were measured using ImageJ 1.51q software. Measurements were made on vessels pairs with a diameter of $d_h \pm 2$ µm (Hacke & Sperry, 2001; Hacke *et al.*, 2001). Values were averaged per plant organ (± SE).

Statistics

For vulnerability analyses, PLC was plotted vs the corresponding Ψ and a Weibull regression curve was fitted to each vulnerability curve (R package fit-plc, R i386 3.2.5; Duursma & Choat, 2017). Differences in anatomical (d, d_h, VD and $(t/b)^2$) and hydraulic parameters (K_{st} and K_s) were tested with a two-way analysis of variance (ANOVA) followed by Tukey posthoc comparison and Student's t-test, respectively, after testing for normal distribution and homoscedasticity. For vulnerability analyses, differences between techniques and organs were assessed using 95% confidence intervals obtained via bootstrap resampling. Student's t-tests were performed using Spss v.24.0 (SPSS Inc., Chicago, IL, USA) at a probability level of 5% while bootstrapping was performed in R Studio.

Results

Hydraulic measurements and micro-CT observations

Vulnerability curves obtained with the hydraulic method did not significantly differ between species, though vulnerability thresholds of *A. pseudoplatanus* were overall higher than of *F. sylvatica* (Ψ_{50} −2.81 MPa vs −3.36 MPa; Fig. 3; Table 1). Micro-CT *in vivo* visualisation of stems confirmed this finding, whereby differences in thresholds were smaller (e.g. Ψ_{50} −2.51 MPa vs −2.74 MPa for *A. pseudoplatanus* and *F. sylvatica*, respectively; Fig. 3; Table 1). Also, vulnerability thresholds did not significantly differ between methods (Fig. 3; Table 1). In both species, calculated stem K_{st} was higher than the measured stem hydraulic conductivity K_s (Table 2).

Micro-CT also revealed similar Ψ_{50} in roots of study species (Table 1). In *A. pseudoplatanus*, *in vivo* visualisation indicated petioles (Ψ_{50} −1.13 MPa) to be more vulnerable than both roots and stems (Fig. 4; Table 1), while roots and stems did not differ in Ψ_{50}. However, roots exhibited significantly higher Ψ_{88} than stems (−2.08 MPa vs −4.69 MPa) with a steep increase in PLC upon decreasing Ψ (Fig. 4e). In petioles, Ψ_{12} could not be determined, because data points at high Ψ were missing. Petiole K_{st} was lower than root and stem K_{st}, which showed similar values (Table 2). In *F. sylvatica*, vulnerability to drought-induced xylem embolism of stems, roots and leaf veins did not differ (Fig. 4b,d, f; Table 1). Main leaf vein K_{st} was higher than root K_{st}, which was higher than stem K_{st} (Table 2).

Anatomical parameters

Both species showed similar stem d and d_h (Table 2), whereby in *A. pseudoplatanus* the size of most frequent conduits was smaller and a fraction of large diameter conduits (> 38 µm) present, which were missing in *F. sylvatica* (Fig. 5). In *A. pseudoplatanus*, leaf and root xylem showed significantly smaller d and d_h values (Table 2) than in *F. sylvatica*.

In *A. pseudoplatanus*, pronounced differences in the number of larger conduits (> 20 µm) were observed between organs (Fig. 5a, c,e). In petioles, d and d_h were smaller than in roots, while largest d and d_h were found in stems (Table 2; see also Fig. 5). In *F. sylvatica*, d_h of roots (23.72 ± 0.67 µm) and stems (22.65 ± 1.09 µm) was similar (see Table 2) while d and diametric classes distribution differed (Fig. 5d,f; Table 2). Major leaf veins of *F. sylvatica* showed smaller d and d_h (Table 2; see also Fig. 5) than roots and stems.

Both species showed low stem VD when compared with roots and leaf veins/petioles (Table 2). In *A. pseudoplatanus*, root and petiole VD did not differ, while leaf veins had a significantly higher VD than roots in *F. sylvatica*. Cell-wall reinforcement $(t/b)^2$ showed minor variation in *A. pseudoplatanus*. In *F. sylvatica*, stems exhibited higher $(t/b)^2$ values than both roots and leaf (Table 2).

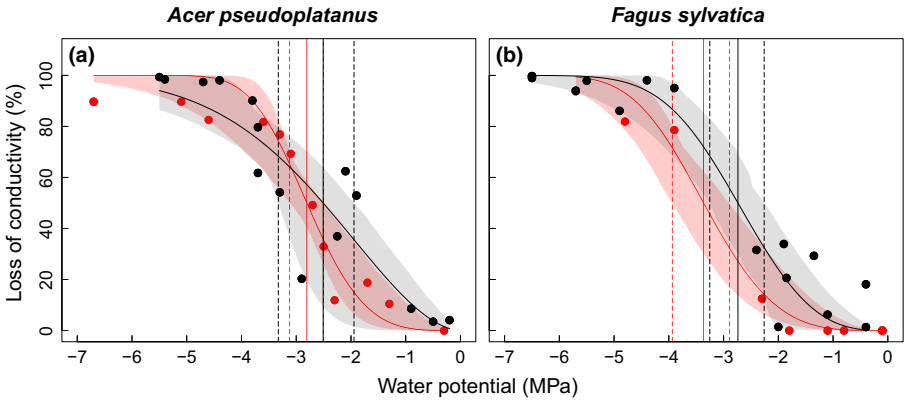

Fig. 3 Vulnerability to drought-induced xylem embolism from hydraulic measurements (red) and micro-CT observations (black) of stems of *Acer pseudoplatanus* (a) and *Fagus sylvatica* (b) seedlings. Solid vertical lines represent water potential at 50% loss of conductivity (Ψ_{50}), dashed vertical lines represent lower and upper confidence intervals for Ψ_{50}. Shaded areas represent the 95% bootstrapped confidence interval for fitted curves.

Table 1 Vulnerability to drought-induced embolism of *Acer pseudoplatanus* and *Fagus sylvatica* stems, roots and leaves obtained with hydraulic measurements and micro-CT observations.

Species	Ψ_{12}, MPa	CI 2.5%	CI 97.5%	Ψ_{50}, MPa	CI 2.5%	CI 97.5%	Ψ_{88}, MPa	CI 2.5%	CI 97.5%	*n*
A. pseudoplatanus										
Hydraulic (stem)	−1.83 a	−1.07	−2.17	−2.81 a	−2.54	−3.13	−3.72 a	−3.44	−5.04	13
Micro-CT (petiole)				−1.13 b*	−0.96	−1.32	−3.01 b	−2.35	−3.54	10
Micro-CT (stem)	−0.97 a	−0.56	−2.6	−2.51 a	−1.93	−3.33	−4.69 a	−3.78	−5.69	15
Micro-CT (root)	−1.41 a	−1.39	−2.18	−1.78 a	−1.77	−2.48	−2.08 b	−1.97	−2.7	10
F. sylvatica										
Hydraulic (stem)	−2.16 a	−1.37	−2.65	−3.36 a	−2.92	−3.94	−4.52 a	−4.15	−5.27	9
Micro-CT (leaf main vein)	−1.30 a	−0.67	−3.02	−2.26 a	−1.93	−3.31	−3.25 a	−2.53	−5.15	12
Micro-CT (stem)	−1.54 a	−0.93	−2.26	−2.74 a	−2.28	−3.24	−4.00 a	−3.09	−5.11	16
Micro-CT (root)	−1.73 a	−1.16	−2.32	−2.75 a	−2.00	−3.33	−3.74 a	−2.07	−4.77	8

Parameters Ψ_{12}, Ψ_{50} and Ψ_{88} correspond to Ψ at 12, 50 and 88% loss of conductivity, respectively, and CI 2.5% and CI 97.5% indicate the confidence interval for each parameter. *n*, the number of samples used for plotting each vulnerability curve. Letters indicate statistically significant differences in the respective parameter within a species, asterisks between species ($P < 0.05$).

Table 2 Mean conduit diameter (d), mean vessel hydraulic diameter (d_h), vessel density (VD), cell-wall reinforcement $(t/b)^2$ and mean theoretical specific hydraulic conductivity (K_{st}) of roots, stems and leaves, and mean specific hydraulic conductivity (K_s) of stems of *Acer pseudoplatanus* and *Fagus sylvatica* seedlings.

Species	Organ	d (μm)	d_h (μm)	VD (n mm^{-2})	$(t/b)^2$	K_{st} (kg m^{-1} MPa^{-1} s^{-1})	K_s (kg m^{-1} MPa^{-1} s^{-1})
A. pseudoplatanus	Root	11.15 ± 1.13 a*	15.63 ± 0.71 a*	1284.0 ± 2.6 a*	0.083 ± 0.006 a	0.95 ± 0.13 a*	
	Stem	17.24 ± 1.50 b	25.06 ± 1.89 b	211.5 ± 0.8 b*	0.070 ± 0.008 a*	0.95 ± 0.16 a	0.14 ± 0.01**
	Petiole	10.47 ± 0.23 a*	13.96 ± 0.26 a*	908.3 ± 1.1 a	0.063 ± 0.006 a	0.76 ± 0.18 a*	
F. sylvatica	Root	14.51 ± 1.44 a	22.65 ± 1.09 a	741.3 ± 2.1 a	0.080 ± 0.009 a	2.01 ± 0.24 a	
	Stem	18.36 ± 0.64 b	23.72 ± 0.67 a	314.4 ± 0.6 b	0.140 ± 0.004 b	1.35 ± 0.13 b	0.34 ± 0.05**
	Main leaf vein	12.01 ± 1.25 a	16.42 ± 0.88 b	2551.3 ± 3.9 c	0.074 ± 0.018 a	2.51 ± 0.60 a	

Letters indicate statistically significant differences in the respective parameter within a species, asterisks between species ($P < 0.05$). Double asterisks indicate significant differences between K_{st} and K_s within a species ($P < 0.05$). Mean ± SE.

Discussion

Based on the micro-CT technique, xylem resistance to drought-induced embolism in seedlings of two angiosperm species could be studied *in vivo*. The experimental design enabled the analysis of vulnerabilities in different organs of individual plants. Micro-CT observations demonstrated within-plant variation in the vulnerabilities of one out of two study species and thus species-specificity in the hydraulic architecture of seedlings. Moreover, comparison of micro-CT observations and hydraulic measurements indicated agreement between methods.

Micro-CT scans enabled the analysis of within-plant patterns in hydraulic traits at small scale. In the present study, this technique was used to compare the hydraulic vulnerability of stem, roots and leaves within intact seedlings, which had an age of only few months, while previous studies dealt with either saplings or detached organs of adult trees (e.g. Choat *et al.*, 2015, 2016; Cochard *et al.*, 2015; Bouche *et al.*, 2016; Cuneo *et al.*, 2016; Knipfer *et al.*, 2016, 2017; Ryu *et al.*, 2016; Nardini *et al.*, 2017; Nolf *et al.*, 2017; Scoffoni *et al.*, 2017). Interestingly, the mean vulnerability of seedling stems was lower than that of branches from adult trees of *A. pseudoplatanus* (Ψ_{50} −1.60 and −2.2 MPa from Tissier *et al.*, 2004 and Lens *et al.*, 2011; respectively). In 2-yr-old saplings, Lübbe *et al.* (2017) also found lower Ψ_{50} (*c.* −3.70 MPa) compared with branches of adult trees (Tissier *et al.*, 2004; Lens *et al.*, 2011). In contrast, *F. sylvatica* seedlings showed a stem Ψ_{50} similar to adult trees and to 2-yr-old saplings (Lübbe *et al.*, 2017; Bär *et al.*, 2018). This indicates that early ontogenetic stages of *A. pseudoplatanus* are probably better protected against drought-induced xylem dysfunction than adult trees, which may be necessary to counterbalance the small root system (see 'Introduction'). For *F. sylvatica* seedlings, this aspect may be less relevant due to this species' overall lower hydraulic vulnerability and its shade tolerance. *F. sylvatica* is a very shade-tolerant and heavy shade-casting species (Petritan *et al.*, 2007) and may be better protected in the understory from risky transpirational losses. Though, the recorded Ψ_{88} was less negative than in 2-yr-old saplings in both species (−6.00 and −4.80 MPa for *A. pseudoplatanus* and *F. sylvatica*, respectively; Lübbe *et al.*, 2017). Intense drought events thus might produce significantly larger impacts and mortality in seedlings. However, comparison of vulnerability thresholds of our seedlings with mature trees analysed in previous studies have to be taken with caution as different methods and techniques were used.

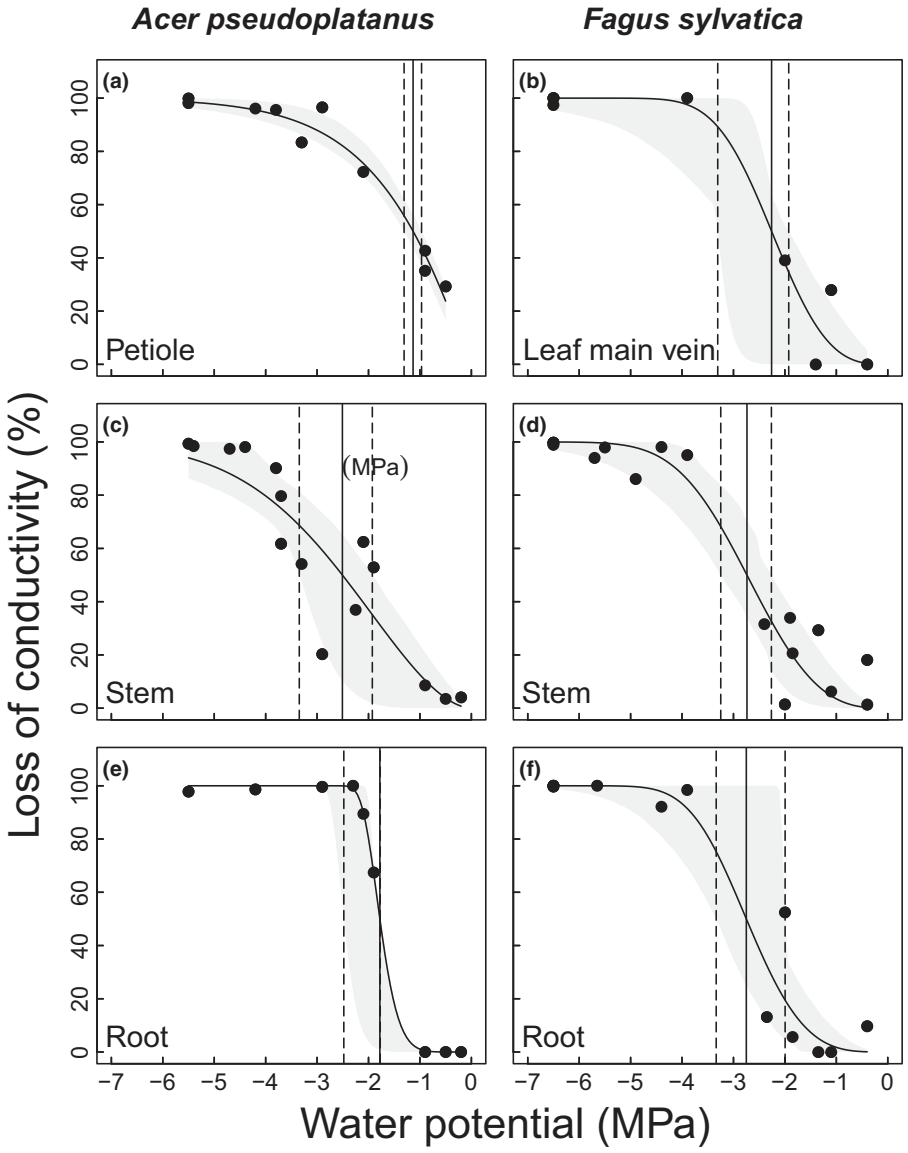

Fig. 4 Vulnerability to drought-induced xylem embolism of micro-CT observations of leaves (a, b), stems (c, d) and roots (e, f) of *Acer pseudoplatanus* and *Fagus sylvatica* seedlings. Solid vertical lines represent water potential at 50% loss of conductivity (Ψ_{50}), dashed vertical lines represent lower and upper confidence intervals for Ψ_{50}. Grey shaded areas represent the 95% bootstrapped confidence interval for fitted curves. Stem curves are also shown in Fig. 3.

Petioles of *A. pesudoplatanus* (Fig. 4a) were found to be more vulnerable than both stems and roots, while in *F. sylvatica*, organs exhibited similar vulnerabilities (Fig 3d,f,h; Table 1). It should be noticed that leaf vulnerability analyses considered only xylary pathways (in petioles or main veins) but not extra-xylary components (Trifilò *et al.*, 2016; Scoffoni *et al.*, 2017). Recent studies on angiosperm species (Klepsch *et al.*, 2018; Wason *et al.*, 2018) also reported leaf xylem to be similarly resistant to embolism compared with other organs except for *Acer rubrum* (Wason *et al.*, 2018), which exhibited more vulnerable petioles than stems. Interestingly, in roots of *A. pseudoplatanus*, Ψ_{12} and Ψ_{50} were similar to stems, while Ψ_{88} was less negative (Fig. 4c, e; Table 1). This indicates resistance of roots to moderate drought, which likely can occur in upper soil layers. Rodriguez-Dominguez *et al.* (2018) found roots of *Olea europaea* saplings to have more resistant xylem than stems and leaves, and Tsuda & Tyree (1997) reported higher hydraulic safety in roots compared with stems in *A. saccharinum* saplings. In contrast, several studies indicated fine roots to exhibit low hydraulic safety and thus to act as hydraulic 'fuses' (Jackson *et al.*, 2000; Cuneo *et al.*, 2016). Though, the present micro-CT study focused on the seedlings' main root, which (although similar in size) may differ from fine roots.

During the dehydration process, leaves of both species under study started to wilt below distinct Ψ. This was particularly pronounced in *A. pseudoplatanus*, which suffered severe wilting at Ψ of *c.* −1 to −1.5 MPa. Wilting thus happened before Ψ_{50} was reached, even in *A. pseudoplatanus*, whose petioles showed the highest vulnerability in this study. As suggested by other authors (Tyree *et al.*, 1993; Pivovaroff *et al.*, 2014; Savi *et al.*, 2016; Wolfe *et al.*, 2016), leaf wilting and shedding might play an important role under drought stress by reducing transpiration and water loss. Embolism formation in the leaf petiole and/or leaf veins is expected to further disconnect the main stem from leaves and thus delay the decrease of stem Ψ and the risk of xylem dysfunction. Under drought, a timely onset of these protective

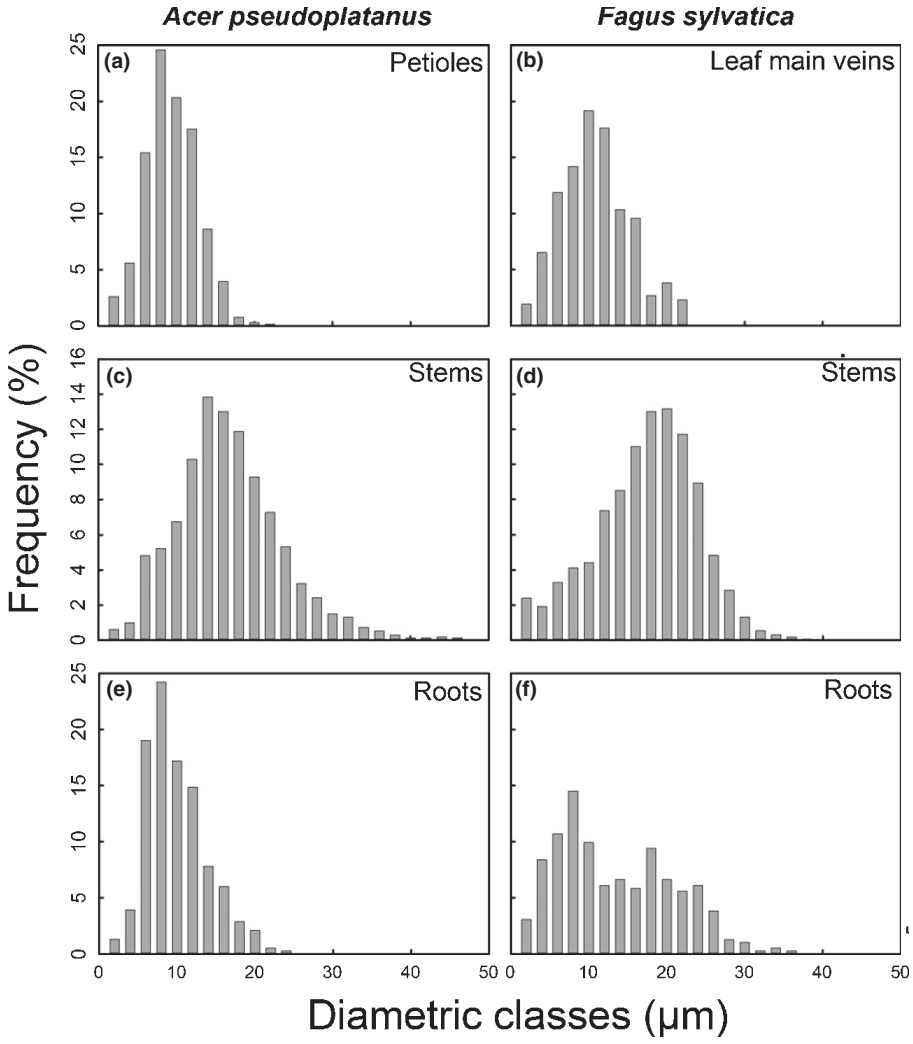

Fig. 5 Distribution of conduit diameters (2 µm classes) of stems (a, b), roots (c, d) and leaves (e, f) of *Acer pseudoplatanus* (a, c, e) and *Fagus sylvatica* (b, d, f) seedlings.

mechanisms may be essential to guarantee survival in young seedlings.

Anatomical parameters (i.e. d, d_h, VD and $(t/b)^2$) were overall similar between organs (Table 2) and hardly reflected observed variations in hydraulic vulnerability. In *A. pseudoplatanus*, no difference in conduit size (d and d_h) or VD between petioles and roots were observed, while the stem exhibited wider conduits but lower VD. Similar values of $(t/b)^2$, which is related to the hydraulic vulnerability (e.g. Hacke & Sperry, 2001; Hacke *et al.*, 2001), were recorded across organs. In *A. rubrum*, Wason *et al.* (2018) reported similar hydraulic safety across organs despite differences in conduit diameters. In *F. sylvatica*, despite the absence of differences in hydraulic vulnerability, stems exhibited wider conduits, lower VD and lower $(t/b)^2$ than roots and leaf main veins. These veins showed the highest VD values as conduits were smaller in size and grouped in bundles. We suppose that mechanical demands substantially influenced the measured anatomical parameters and masked possible hydraulic structure-function relationships. Also, the properties of pits, which are central structures with respect to drought-induced xylem dysfunction (e.g. Cochard *et al.*, 2009; Lens *et al.*, 2011; Li *et al.*, 2016), were not considered in our study but relevant as indicated by the differences between K_{st} calculated form micro-CT images and hydraulically measured K_s. More studies, ideally based on micro-CT analysis at higher resolution, would be desirable to investigate the relation between pit characteristics and hydraulic vulnerability segmentation in more detail.

In both species under study, stem vulnerability curves based on hydraulic measurements were similar to those obtained with micro-CT observations. These results agree with previous studies (e.g. Nardini *et al.*, 2017; Nolf *et al.*, 2017) and indicate that, when appropriate precaution is taken, 'cutting artefacts' (Wheeler *et al.*, 2013) do not bias hydraulic measurements by causing an overestimation of vulnerability. The Ψ_{50} of hydraulic curves was even more negative than Ψ_{50} obtained with micro-CT (Fig. 3; Table 1), as also reported by Savi *et al.* (2017) for young sunflower stems. This difference between methods can be attributed to three main methodological limitations: (1) Micro-CT observations can lead to an overestimation of conductivity, when conduits are water filled but do not contribute to sap flow. This may be the case when conduits are not connected to adjacent ones (e.g. due to immature conduits). (2) Micro-CT only allows an

estimation of conductivities based on conduit diameter, and calculations do neither include pit resistances nor resistances caused by the cell walls. (3) Hydraulic measurements on small plant material are difficult and may not be highly accurate due to e.g. conduit clogging, cut open vessels, accidental removal of embolism during sample preparation and gas exsolution. Accordingly, hydraulic vulnerability measurements never showed a PLC higher than 95%, while in micro-CT observations, 100% PLC were reached already at −4.5 MPa (see Fig. 3). In a recent study, Savi *et al.* (2017) suggested that higher rates of PLC in micro-CT based vulnerability curves might be caused by the exposition of samples to heat and/or X-ray absorption during sample alignment and scanning. However, in our study, samples were not exposed to irradiation during the initial alignment and the scan time was rather short (90 s) compared with other studies (Cochard *et al.*, 2015; Choat *et al.*, 2016; Knipfer *et al.*, 2016; Ryu *et al.*, 2016; Nardini *et al.*, 2017; Nolf *et al.*, 2017).

Further analyses on larger species pools and on wider spatial scales (e.g. including fine roots), as well as a combination with other important hydraulic and physiological traits (e.g. water storage, leaf shedding) will be essential to better understand water relations of trees at early ontogenetic stages. Improved knowledge on seedling hydraulics will be an important base to optimise afforestation strategies and future management under climate change projections of progressively warmer and drier conditions.

Acknowledgements

This study was made possible by Elettra-Sincrotrone Trieste, which allowed and funded access to the SYRMEP beamline (proposal no. 20165277). We thank the technical staff at SYRMEP for the assistance during experiments, Walter Steger for help with construction of the sample holder and Markus Bodner for help with growing the seedlings. The study was also supported by the Austrian research agency (FWF), project T667-B16 Hydraulics of juvenile trees and project P29896-B22 Analysis of Norway spruce rust-resistance, and by a Sparkling Science Project SPA 05/017 funded by the Federal Ministry of Science, Research, and Economy (Bundesministerium für Wissenschaft, Forschung, und Wirtschaft) Austria.

Author contributions

BB, SM and AL planned and designed the present study. AL performed hydraulic experiments. AL, AB, BD, CD, AG, FP, TS, GT, SM and AN were involved in micro-CT observations. Important technical support was given by GT, FP and CD. AL and AG made the image reconstruction. AL, AB, AG, BB, SM and AN performed data analyses and interpretation. The manuscript was prepared by AL, SM and BB with contributions from all other authors.

References

Bär A, Nardini A, Mayr S. 2018. Post-fire effects in xylem hydraulics of *Picea abies*, *Pinus sylvestris* and *Fagus sylvatica*. *New Phytologist* **217**: 1484–1493.

Beikircher B, De Cesare C, Mayr S. 2013. Hydraulics of high-yield orchard trees: a case study of three *Malus domestica* cultivars. *Tree Physiology* **33**: 1296–1307.

Beikircher B, Mayr S. 2008. The hydraulic architecture of *Juniperus communis* L. ssp. communis: shrubs and trees compared. *Plant, Cell & Environment* **31**: 1545–1556.

Beikircher B, Mayr S. 2009. Intraspecific differences in drought tolerance and acclimation in hydraulics of *Ligustrum vulgare* and *Viburnum lantana*. *Tree Physiology* **29**: 765–775.

Boehm J. 1893. Capillarität und Saftsteigen. *Berichte der Deutschen Botanischen Gesellschaft* **11**: 203–212.

Bouche PS, Delzon S, Choat B, Badel E, Brodribb TJ, Burlett R, Cochard H, Charra-Vaskou K, Lavigne B, Li S *et al.* 2016. Are needles of *Pinus pinaster* more vulnerable to xylem embolism than branches? New insights from X-ray computed tomography. *Plant, Cell & Environment* **39**: 860–870.

Brodersen CR, MacElron AJ, Choat B, Lee EF, Shackel KA, Matthews MA. 2013. *In vivo* visualizations of drought-induced embolism spread in *Vitis vinifera*. *Plant Physiology* **161**: 1820–1829.

Brodribb TJ, Cochard H. 2009. Hydraulic failure defines the recovery and point of death in water-stressed conifers. *Plant Physiology* **149**: 575–584.

Brodribb TJ, Skelton RP, McAdam SAM, Bienaimé D, Lucani CJ, Marmottant P. 2016. Visual quantification of embolism reveals leaf vulnerability to hydraulic failure. *New Phytologist* **209**: 1403–1409.

Brun F, Pacilè S, Accardo A, Kourousias G, Dreossi D, Mancini L, Pugliese R. 2015. Enhanced and flexible software tools for X-ray computed tomography at the Italian Synchrotron Radiation Facility Elettra. *Fundamenta Informaticae* **141**: 233–243.

Charrier G, Torres-Ruiz JM, Badel E, Burlett R, Choat B, Cochard H, EL Delmas C, Domec J-C, Jansen S, King A *et al.* 2016. Evidence for hydraulic vulnerability segmentation and lack of xylem refilling under tension. *Plant Physiology* **172**: 1657–1668.

Choat B, Badel E, Burlett R, Delzon S, Cochard H, Jansen S. 2016. Noninvasive measurement of vulnerability to drought-induced embolism by X-ray microtomography. *Plant Physiology* **170**: 273–282.

Choat B, Brodersen CR, Mcelrone AJ. 2015. Synchrotron X-ray microtomography of xylem embolism in *Sequoia sempervirens* saplings during cycles of drought and recovery. *New Phytologist* **205**: 1095–1105.

Choat B, Drayton WM, Brodersen C, Matthews MA, Shackel KA, Wada H, McElrone AJ. 2010. Measurement of vulnerability to water stress-induced cavitation in grapevine: a comparison of four techniques applied to a long-vesseled species. *Plant, Cell & Environment* **33**: 1502–1512.

Choat B, Jansen S, Brodribb TJ, Cochard H, Delzon S, Bhaskar R, Bucci SJ, Feild TS, Gleason SM, Hacke UG *et al.* 2012. Global convergence in the vulnerability of forests to drought. *Nature* **491**: 752–755.

Choat B, Lahr EC, Melcher PJ, Zwieniecki MA, Holbrook NM. 2005. The spatial pattern of air seeding thresholds in mature sugar maple trees. *Plant, Cell & Environment* **28**: 1082–1089.

Cochard H, Badel E, Herbette S, Delzon S, Choat B, Jansen S. 2013. Methods for measuring plant vulnerability to cavitation: a critical review. *Journal of Experimental Botany* **64**: 4779–4791.

Cochard H, Delzon S, Badel E. 2015. X-ray microtomography (micro-CT): a reference technology for high-resolution quantification of xylem embolism in trees. *Plant, Cell & Environment* **38**: 201–206.

Cochard H, Hölttä T, Herbette S, Delzon S, Mencuccini M. 2009. New insights into the mechanisms of water-stress-induced cavitation in conifers. *Plant Physiology* **151**: 949–954.

Cuneo IF, Knipfer T, Brodersen CR, McElrone AJ. 2016. Mechanical failure of fine root cortical cells initiates plant hydraulic decline during drought. *Plant Physiology* **172**: 1669–1678.

Delzon S, Douthe C, Sala A, Cochard H. 2010. Mechanism of water-stress induced cavitation in conifers: bordered pit structure and function support the hypothesis of seal capillary-seeding. *Plant, Cell & Environment* **33**: 2101–2111.

Dixon H, Joly J. 1894. On the ascent of sap. *Annals of Botany* **8**: 468–470.

Domec J-C, Gartner BL. 2001. Cavitation and water storage capacity in bole xylem segments of mature and young Douglas-fir trees. *Trees - Structure and Function* **15**: 204–214.

Domec J-C, Warren JM, Meinzer FC, Lachenbruch B. 2009. Safety factors from air seeding and cell wall implosion in young and old conifer trees. *IAWA Journal* **30**: 100–120.

Duursma RA, Choat B. 2017. fitplc-an R package to fit hydraulic vulnerability curves. *Journal of Plant Hydraulics* **4**: 002.

Fenner M. 1987. Seedlings. *New Phytologist* **106**: 35–47.

Ganthaler A, Mayr S. 2015. Dwarf shrub hydraulics: two *Vaccinium* species (*Vaccinium myrtillus*, *Vaccinium vitis-idaea*) of the European Alps compared. *Physiologia Plantarum* **4**: 424–434.

Gleason SM, Westoby M, Jansen S, Choat B, Hacke UG, Pratt RB, Bhaskar R, Brodribb TJ, Bucci SJ, Cao K-F *et al.* 2016. Weak tradeoff between xylem safety and xylem-specific hydraulic efficiency across the world's woody plant species. *New Phytologist* **209**: 123–136.

Grulke NE, Retzlaff WA. 2001. Changes in physiological attributes of ponderosa pine from seedling to mature tree. *Tree Physiology* **21**: 275–286.

Hacke UG, Sperry JS. 2001. Functional and ecological xylem anatomy. *Perspectives in Plant Ecology, Evolution and Systematics* **4**: 97–115.

Hacke UG, Sperry JS, Pockman WT, Davis SD, McCulloh KA. 2001. Trends in wood density and structure are linked to prevention of xylem implosion by negative pressure. *Oecologia* **126**: 457–461.

Hao GY, Wheeler JK, Holbrook NM, Goldstein G. 2013. Investigating xylem embolism formation, refilling and water storage in tree trunks using frequency domain reflectometry. *Journal of Experimental Botany* **64**: 2321–2332.

Ibanez I, Clark JS, LaDeau S, Hille Ris Lambers J. 2007. Exploiting temporal variability to understand tree recruitment response to climate change. *Ecological Monographs* **77**: 163–177.

Jackson RB, Sperry JS, Dawson TE. 2000. Root water uptake and trans- port: using physiological processes in global predictions. *Trends in Plant Science* **5**: 482–488.

Jansen S, Schuldt B, Choat B. 2015. Current controversies and challenges in applying plant hydraulic techniques. *New Phytologist* **205**: 961–964.

Johnson DM, McCulloh KA, Reinhardt K. 2011. The earliest stages of tree growth: development, physiology and impacts of microclimate. In: Meinzer FC, Lachenbruch B, Dawson TE, eds. *Size- and age-related changes in tree structure and function*. Dordrecht, the Netherlands: Springer, 65–87.

Johnson DM, Wortemann R, McCulloh KA, Jordan-Meille L, Ward E, Warren JM, Palmroth S, Domec J-C. 2016. A test of the hydraulic vulnerability segmentation hypothesis in angiosperm and conifer tree species. *Tree Physiology* **36**: 989–993.

Kavanagh KL, Bond BJ, Aitken SN, Gartner BL, Knowe S. 1999. Shoot and root vulnerability to xylem cavitation in four populations of Douglas-fir seedlings. *Tree Physiology* **19**: 31–37.

Klepsch M, Zhang Y, Kotowska MM, Lamarque L, Nolf M, Schuldt B, Torres-Ruiz JM, Qin D-W, Choat B, Delzon S *et al.* 2018. Is xylem of angiosperm leaves less resistant to embolism than branches? Insights from microCT, hydraulics, and anatomy *Journal of Experimental Botany*. doi: 10.1093/jxb/ery321.

Knipfer T, Cuneo I, Brodersen C, McElrone AJ. 2016. In-situ visualization of the dynamics in xylem embolism formation and removal in the absence of root pressure: a study on excised grapevine stems. *Plant Physiology* **171**: 1024–1036.

Knipfer T, Cuneo I, Earles JM, Reyes C, Brodersen C, McElrone AJ. 2017. Storage compartments for capillary water rarely refill in an intact woody plant. *Plant Physiology* **175**: 1649–1660.

Knipfer T, Eustis A, Brodersen C, Walker AM, McElrone AJ. 2015. Grapevine species from varied native habitats exhibit differences in embolism formation/repair associated with leaf gas exchange and root pressure. *Plant, Cell & Environment* **38**: 1503–1513.

Kolb KJ, Sperry JS. 1999. Differences in drought adaptation between subspecies of sagebrush (*Artemisia Tridentata*). *Ecology* **80**: 2373–2384.

Larcher W 2003. *Physiological plant ecology*. Heidelberg, Germany & New York, NY, USA: Springer Verlag Berlin.

Lauenstein DAL, Fernández ME, Verga AR. 2013. Drought stress tolerance of *Prosopis chilensis* and *Prosopis flexuosa* species and their hybrids. *Trees - Structure and Function* **27**: 285–296.

Lens F, Sperry JS, Christman MA, Choat B, Rabaey D, Jansen S. 2011. Testing hypotheses that link wood anatomy to cavitation resistance and hydraulic conductivity in the genus *Acer*. *New Phytologist* **190**: 709–723.

Li S, Lens F, Espino S, Karimi Z, Klepsch M, Schenck HJ, Schmitt M, Schuldt B, Jansen S. 2016. Intervessel pit membrane thickness as a key determinant of embolism resistance in angiosperm xylem. *IAWA Journal* **37**: 152–171.

Losso A, Nardini A, Dämon B, Mayr S. 2018. Xylem sap chemistry: seasonal changes in timberline conifers *Pinus cembra*, *Picea abies*, and *Larix decidua*. *Biologia Plantarum* **62**: 157–165.

Losso A, Nardini A, Nolf M, Mayr S. 2016. Elevational trends in hydraulic efficiency and safety of *Pinus cembra* roots. *Oecologia* **180**: 1091–1102.

Lübbe T, Schuldt B, Leuschner C. 2017. Acclimation of leaf water status and stem hydraulics to drought and tree neighbourhood: alternative strategies among the saplings of five temperate deciduous tree species. *Tree Physiology* **37**: 456–468.

Maherali H, Moura CF, Caldeira MC, Willson CJ, Jackson RB. 2006. Functional coordination between leaf gas exchange and vulnerability to xylem cavitation in temperate forest trees. *Plant, Cell & Environment* **29**: 571–583.

Martínez-Vilalta J, Prat E, Oliveras I, Piñol J. 2002. Xylem hydraulic properties of roots and stems of nine Mediterranean woody species. *Oecologia* **133**: 19–29.

Mayr S, Sperry JS. 2010. Freeze–thaw-induced embolism in *Pinus contorta*: centrifuge experiments validate the 'thaw-expansion hypothesis' but conflict with ultrasonic emission data. *New Phytologist* **185**: 1016–1024.

McCulloh KA, Johnson DM, Meinzer FC, Woodruff DR. 2014. The dynamic pipeline: hydraulic capacitance and xylem hydraulic safety in four tall conifer species. *Plant, Cell & Environment* **37**: 1171–1183.

Miller ML, Johnson DM. 2017. Vascular development in very young conifer seedlings: theoretical hydraulic capacities and potential resistance to embolism. *American Journal of Botany* **104**: 979–992.

Nardini A, Savi T, Losso A, Petit G, Pacilè S, Tromba G, Mayr S, Lo Gullo MA, Salleo S. 2017. X-ray microtomography observations of xylem embolism in stems of *Laurus nobilis* are consistent with hydraulic measurements of percentage loss of conductance. *New Phytologist* **213**: 1068–1075.

Nolf M, Lopez R, Peters JMR, Flavel RJ, Koloadin LS, Young IM, Choat B. 2017. Visualization of xylem embolism by X-ray microtomography: a direct test against hydraulic measurements. *New Phytologist* **214**: 890–898.

Nolf M, Rosani A, Ganthaler A, Beikircher B, Mayr S. 2016. Herb hydraulics: inter- and intraspecific variation in three *Ranunculus* species. *Plant Physiology* **170**: 2085–2094.

Paganin D, Mayo SC, Gureyev TE, Miller PR, Wilkins SW. 2002. Simultaneous phase and amplitude extraction from a single defocused image of a homogeneous object. *Journal of Microscopy* **206**: 33–40.

Petritan AM, Von Lüpke B, Petritan IC. 2007. Effects of shade on growth and mortality of maple (*Acer pseudoplatanus*), ash (*Fraxinus excelsior*) and beech (*Fagus sylvatica*) saplings. *Forestry* **80**: 397–412.

Petruzzellis F, Pagliarani C, Savi T, Losso A, Cavalletto S, Tromba G, Dullin C, Bär A, Ganthaler A, Miotto A *et al.* 2018. The pitfalls of *in vivo* imaging techniques: evidence for cellular damage caused by synchrotron X-ray computed micro-tomography. *New Phytologist* **220**: 104–110.

Pittermann J, Sperry J. 2003. Tracheid diameter is the key trait determining the extent of freezing-induced embolism in conifers. *Tree Physiology* **23**: 907–914.

Pivovaroff AL, Sack L, Santiago LS. 2014. Coordination of stem and leaf hydraulic conductance in southern California shrubs : a test of the hydraulic segmentation hypothesis. *New Phytologist* **203**: 842–850.

Rice KJ, Matzner SL, Byer W, Brown JR. 2004. Patterns of tree dieback in Queensland, Australia: the importance of drought stress and the role of resistance to cavitation. *Oecologia* **139**: 190–198.

Rodriguez-Dominguez CM, Murphy MRC, Lucani C, Brodribb TJ. 2018. Mapping xylem failure in disparate organs of whole plants reveals extreme resistance in olive roots. *New Phytologist* **218**: 1025–1035.

Rosner S, Heinze B, Savi T, Dalla-Salda G. 2018. Prediction of hydraulic conductivity loss from relative water loss: new insights into water storage of tree stems and branches. *Physiologia Plantarum*. doi: 10.1111/ppl.12790.

Ryu J, Hwang BG, Kim YX, Lee SJ. 2016. Direct observation of local xylem embolisms induced by soil drying in intact *Zea mays* leaves. *Journal of Experimental Botany* **67**: 2617–2626.

Savi T, Marin M, Luglio J, Petruzzellis F, Mayr S, Nardini A. 2016. Leaf hydraulic vulnerability protects stem functionality under drought stress in *Salvia officinalis*. *Functional Plant Biology* **43**: 370–379.

Savi T, Miotto A, Petruzzellis F, Losso A, Pacilè S, Tromba G, Mayr S, Nardini A. 2017. Drought-induced embolism in stems of sunflower: a comparison of *in vivo* micro-CT observations and destructive hydraulic measurements. *Plant Physiology and Biochemistry* **120**: 24–29.

Scholz FG, Bucci SJ, Goldstein G. 2014. Strong hydraulic segmentation and leaf senescence due to dehydration may trigger die-back in *Nothofagus dombeyi* under severe droughts: a comparison with the co-occurring *Austrocedrus chilensis*. *Trees - Structure and Function* **28**: 1475–1487.

Scoffoni C, Albuquerque C, Brodersen CR, Townes SV, John GP, Bartlett MK, Buckley TN, Mcelrone AJ, Sack L. 2017. Outside-xylem vulnerability, not xylem embolism, controls leaf hydraulic decline during dehydration. *Plant Physiology* **173**: 1197–1210.

Skelton RP, Brodribb TJ, Choat B. 2017. Casting light on xylem vulnerability in an herbaceous species reveals lack of segmentation. *New Phytologist* **214**: 561–569.

Smith WK, Germino MJ, Hancock TE, Johnson DM. 2003. Another perspective on altitudinal limits of alpine timberlines. *Tree Physiology* **23**: 1101–1112.

Sperry JS, Donnelly JR, Tyree MT. 1988. A method for measuring hydraulic conductivity and embolism in xylem. *Plant, Cell & Environment* **11**: 35–40.

Sperry JS, Love DM. 2015. What plant hydraulics can tell us about responses to climate-change droughts. *New Phytologist* **207**: 14–27.

Steudle E. 2001. The cohesion-tension mechanism and the acquisition of water by plant roots. *Annual Review of Plant Physiology* **52**: 847–875.

Tissier J, Lambs L, Peltier J-P, Marigo G. 2004. Relationships between hydraulic traits and habitat preference for six *Acer* species occurring in the French Alps. *Annals of Forest Science* **61**: 81–86.

Trifilò P, Raimondo F, Lo Gullo MA, Barbera PM, Salleo S, Nardini A. 2014. Relax and refill: xylem rehydration prior to hydraulic measurements favours embolism repair in stems and generates artificially low PLC values. *Plant, Cell & Environment* **37**: 2491–2499.

Trifilò P, Raimondo F, Savi T, Lo Gullo MA, Nardini A. 2016. The contribution of vascular and extra-vascular water pathways to drought-induced decline of leaf hydraulic conductance. *Journal of Experimental Botany* **67**: 5029–5039.

Tromba G, Longo R, Abrami A, Arfelli F, Astolfo A, Bregant P, Brun F, Casarin K, Chenda V, Dreossi D *et al.* 2010. *The SYRMEP Beamline of Elettra*. AIP Conference Proceedings, Vol. 1266: 18–23.

Tsuda M, Tyree MT. 1997. Whole-plant hydraulic resistance and vulnerability segmentation in *Acer saccharinum*. *Tree Physiology* **17**: 351–357.

Tyree MT, Cochard H, Cruiziat P, Sinclair B, Ameglio T. 1993. Drought-induced leaf shedding in walnut: evidence for vulnerability segmentation. *Plant, Cell & Environment* **16**: 879–882.

Tyree MT, Davis SD, Cochard H. 1994. Biophysical perspectives of xylem evolution – is there a tradeoff of hydraulic efficiency for vulnerability to dysfunction. *IAWA Journal* **15**: 335–360.

Tyree MT, Ewers FW. 1991. The hydraulic architecture of trees and other woody plants. *New Phytologist* **119**: 345–360.

Tyree MT, Zimmermann MH. 2002. *Plant structures: xylem structure and the ascent of sap*. Berlin, Germany: Springer.

Vanderwel MC, Lyutsarev VS, Purves DW. 2013. Climate-related variation in mortality and recruitment determine regional forest-type distributions. *Global Ecology and Biogeography* **22**: 1192–1203.

Venturas MD, MacKinnon ED, Jacobsen AL, Pratt RB. 2015. Excising stem samples underwater at native tension does not induce xylem cavitation. *Plant, Cell & Environment* **38**: 1060–1068.

Wason JW, Anstreicher KS, Stephansky N, Huggett BA, Brodersen CR. 2018. Hydraulic safety margins and air-seeding thresholds in roots, trunks, branches and petioles of four northern hardwood trees. *New Phytologist* **219**: 77–88.

Way DA, Domec J-C, Jackson RB. 2013. Elevated growth temperatures alter hydraulic characteristics in trembling aspen (*Populus tremuloides*) seedlings: implications for tree drought tolerance. *Plant, Cell & Environment* **36**: 103–115.

Wheeler JK, Huggett BA, Tofte AN, Rockwell FE, Holbrook NM. 2013. Cutting xylem under tension or supersaturated with gas can generate PLC and the appearance of rapid recovery from embolism. *Plant, Cell & Environment* **36**: 1938–1949.

Willson CJ, Manos PS, Jackson RB. 2008. Hydraulic traits are influenced by phylogenetic history in the drought-resistant, invasive genus *Juniperus* (Cupressaceae). *American Journal of Botany* **95**: 299–314.

Wolfe BT, Sperry JS, Kursar TA. 2016. Does leaf shedding protect stems from cavitation during seasonal droughts? A test of the hydraulic fuse hypothesis. *New Phytologist* **212**: 1007–1018.